

New photoacoustic cell design for studying aqueous solutions and gels

J. Kottmann,^{a)} J. M. Rey, and M. W. Sigrist^{b)}

ETH Zurich, Institute for Quantum Electronics, Schafmattstrasse 16, 8093 Zurich, Switzerland

(Received 1 April 2011; accepted 14 July 2011; published online 12 August 2011)

A new photoacoustic (PA) cell design, which is particularly suitable for investigations of liquids, gels, and outgassing samples is presented. The setup is based on a PA cell of only 78.5 mm³ volume, which is sealed on the sample side with either a 163 μm thick chemical vapor deposition diamond window or a 3.91 μm thin diamond membrane. This design offers great advantages compared to traditionally used open-ended PA cells especially when investigating volatile compounds. The new PA cell design is particularly interesting in the studies of biological samples characterized by a high water content. The performance was demonstrated with mid-infrared PA measurements of glucose in aqueous solutions using a tunable quantum-cascade laser as a light source. A detection limit of 100 mg/dl (SNR = 3) has been achieved. Furthermore, the spectral changes of glucose dissolved in water caused by mutorotation have been monitored time-resolved. © 2011 American Institute of Physics. [doi:10.1063/1.3622154]

I. INTRODUCTION

Photoacoustic (PA) cells, used to study solid samples, are usually constructed as open-ended,^{1–4} which implies that the PA chamber is at one end sealed by the sample itself. This causes problems when investigating solid samples containing volatile components since released volatiles lead to varying conditions inside the PA chamber. Laser irradiation of the sample can further increase the outgassing process and results in the changes in light absorption, relative humidity, temperature, and viscosity of the coupling gas. These variations within the PA chamber cause not only undesired fluctuations of the cell signal but also may affect the responsivity of the acoustic detector, which inhibits the generation of stable PA signals. The evaporating components may sometimes reach even the saturation stage after which they condense at the cell walls or at the entrance window, making PA measurements impossible. A further limitation of an open-ended cell is the difficulty encountered when studying liquid samples which do not ensure a rigid sealing at the sample surface (i.e., the cell volume and the sample surface may vary).

An often employed variation of the above described design is referred to as open photoacoustic cell.^{5–7} In this technique the air chamber is omitted and the sample is directly placed on an electret microphone. Only the small air volume within the microphone then serves as transducer medium. However, this approach does not solve the problem of released volatile components and, moreover, is limited to a configuration, where the excitation beam and the detection system are on the different sides of the sample.

Another commonly used PA cell design encloses the sample inside the PA chamber.^{8–10} This technique suffers from the same problems as the open-ended PA cell. In addition, it is unpractical because the PA cell has to be dismantled

every time prior exchanging the sample, which makes it unsuitable for *in situ* applications.

An elegant approach how to deal with variations of the coupling gas, laser power fluctuations and volume changes of the PA chamber has been proposed by Julliard and co-workers.¹¹ They modulated a continuous wave CO₂ laser at two different frequencies using two mechanical choppers. One modulation frequency was kept high to ensure the production of a PA signal proportional to the absorption coefficient α (see Sec. II), whereas the other frequency was adjusted to a much lower value to produce a saturated PA signal (i.e., independent of α). By taking the ratio of the two PA signals, a signal proportional to α and independent of laser intensity, gas volume, temperature, pressure, and gas parameters is obtained. However, this approach can be applied only in situations when the requirements imposed on the choice of the above mentioned two frequency regimes can be met for the sample of interest. Such a technique, developed in the perspective of an application in the beverage industry, has achieved a detection limit of glucose dissolved in water of 500 mg/dl.

Several research groups^{12–16} use a thin metal foil to close the PA cell ensuring, thereby, stable conditions in the PA chamber when studying aqueous solutions. The sample of the interest is brought in good thermal contact with the metal foil outside the PA chamber. The modulated light gets entirely absorbed by the metal foil, and—depending on the heat dissipation to the sample—produces stronger or weaker PA signals. This approach ensures stable conditions inside the PA chamber but does not generate a PA signal directly in the sample of interest. Hence, only the thermal properties and not the optical properties of the sample can be investigated with this method.

An interesting technique for the investigation of optically opaque liquids is the so-called optothermal window.^{17–20} In this approach, the temperature increase in a thin optical window (usually sapphire) in direct contact with the sample of interest is detected piezoelectrically. Since the technique does not need a PA chamber, the release of volatile

^{a)}Electronic mail: kjonas@phys.ethz.ch.

^{b)}Electronic mail: sigrist@iqe.phys.ethz.ch.

components does not disturb the detection. Unfortunately, sapphire is transparent up to $5 \mu\text{m}$ only and hence not applicable for investigations around $10 \mu\text{m}$. The use of an alternative material, transparent in the mid-infrared (MIR) light, which can be produced in thin disk form and at the same time possesses a high thermal expansion coefficient has, to our knowledge, not been reported in literature.

None of the above described techniques offers an appropriate solution when exploring the optical and thermal properties of liquids, gels, and outgassing samples. Varying conditions in the PA chamber are particularly problematic when irradiating biological samples characterized by a high water content with the MIR light, which is strongly absorbed by water. Here, we present a new PA cell design sealed with a diamond cover and compare it with an open-ended cell. The PA cell performance is illustrated by detecting glucose in aqueous solutions and by monitoring the temporal spectral changes of glucose dissolved in water caused by mutorotation.

II. GENERAL CONSIDERATION ON PA SIGNAL GENERATION AND DETECTION

Often, biological samples are characterized by their high water content. When irradiated by the MIR light, these samples are usually optically thick (i.e., sample length $l >$ optical penetration depth $\mu_a = 1/\alpha$) because of the strong water absorption in this wavelength region. If the modulation frequency f of the laser is kept in a regime such that

$$\mu_a > \mu_s = \left(\frac{D_s}{\pi \times f} \right)^{\frac{1}{2}}, \quad (1)$$

where μ_s is the thermal diffusion length and D_s is the thermal diffusivity, the generated PA signal is proportional to the absorption coefficient α . According to the well-known Rosencwaig-Gersho model,²¹ in such cases the PA signal amplitude (A_{PA}) shows the following dependence:

$$A_{\text{PA}} \propto \frac{I \times \alpha}{V \times f^{\frac{3}{2}}}, \quad (2)$$

where I is the intensity of the incoming laser light and V is the volume of the PA chamber. Equation (2) implies that a small size PA chamber and a low modulation frequency are desirable in order to obtain strong PA signals. Varying the modulation frequency enables depth profiling, since μ_s is inversely proportional to $f^{0.5}$ (Eq. (1)). For pure water at room temperature the frequency at which $\mu_a = \mu_s$ is about 200 Hz (Fig. 1), as calculated using the values given in Table I. Hence, a modulation frequency above 200 Hz must be chosen to obtain a linear proportionality between the magnitude of the PA signal and the absorption coefficient.

If the PA cell is sealed on the sample side by means of an optical window, it should be optically transparent and also ensure a good thermal contact with the sample of interest. Although materials such as ZnSe, BaF₂, or Ge are all optically transparent in the MIR, they have only moderate thermal conductivities and are difficult to produce in the form of thin disks or foils. On the other hand, diamond is one of the best thermal conductors and allows the production of very thin optical

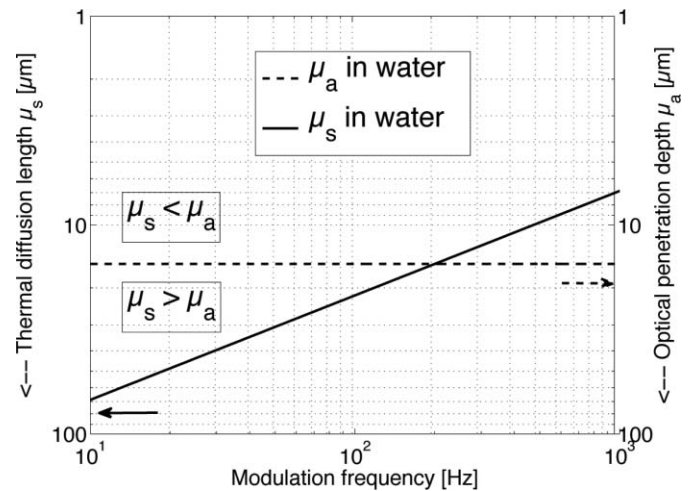


FIG. 1. Frequency dependence of the thermal diffusion length μ_s in water (solid line). A comparison with the minimal optical penetration depth μ_a between 1000 and 1100 cm^{-1} (dashed line) allows a classification into different regimes of PA signal generation.

windows. Due to the progresses in chemical vapor deposition (CVD) techniques the production of large area diamond wafers is possible, which match the properties of the best natural diamonds.²⁴ A CVD diamond of optical grade, as used in this study, has a thermal conductivity of $\sim 1800 \text{ W/mK}$ (see Table I); hence the heat transfer from the sample to the gas in contact with the inner surface of the diamond window (DW) is very efficient. Moreover, diamond has a very high and flat transmission across the broad wavelength range from just beyond the band gap edge at 250 nm to the far infrared, only disturbed by the intrinsic phonon absorption around $5 \mu\text{m}$.²³ These properties combined with its hardness and chemical inertness make the DW very useful for various applications. The high transparency enables an efficient excitation of the sample and causes only a weak PA signal from the window itself (direct window heating). Introducing a thin DW as PA cell window can be thought of as probing a two-layer sample, consisting of an optically and thermally thin diamond layer (i.e., $\mu_s > l_d$ and $\mu_a > l_d$ with l_d being the DW thickness) and the underlying sample of interest. Using the values given in Table I the dependence of the thermal diffusion length μ_s on the modulation frequency for optical grade CVD diamond is plotted in Fig. 2. Due to the high optical penetration depth μ_a of MIR light into diamond ($>65 \text{ mm}$, as indicated by the dashed line), for modulation frequencies between 10 and 1000 Hz, we are in a regime where $\mu_s < \mu_a$. When utilizing a modulation frequency of 200 Hz and a diamond thickness of less than 1.3 mm, the generated thermal wave in the sample

TABLE I. Material constants of water and CVD diamond used for the calculations (Refs. 22 and 23).

Material	Density (kg/m ³)	Thermal conductivity (W/(mK))	Heat capacity (J/(kg K))	α_{max} , 1000–1100 (cm ⁻¹)
Water	997	0.615	4181	651
CVD diamond	3515	1800	502	0.15

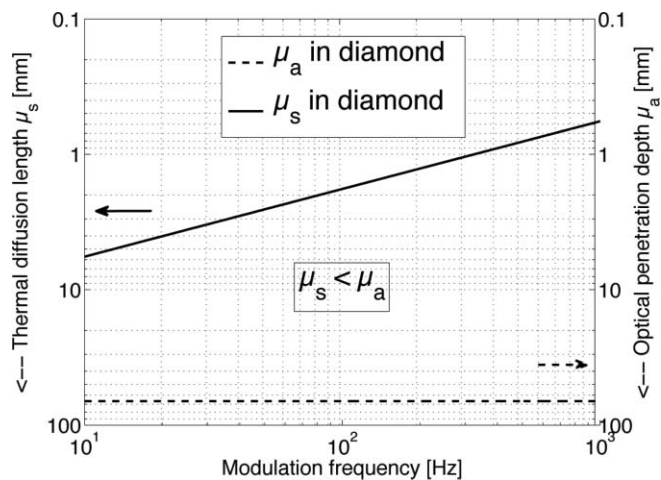


FIG. 2. Frequency dependence of the thermal diffusion length μ_s in diamond (solid line) and the minimal optical penetration depth μ_a between 1000 and 1100 cm^{-1} (dashed line). In this wavelength range modulation frequencies $f > 10$ Hz imply $\mu_s < \mu_a$.

still stimulates the coupling gas because $\mu_s > l_d$ holds. Reducing the thickness of the diamond cover used to seal the PA cell increases the thermal contact and the PA signal generated within the sample. In order to preserve its outstanding thermal properties, no antireflection (AR) coatings were applied to the DW and hence it acts as a Fabry-Perot etalon showing a wavelength-dependent transmission. For diamond with a refractive index of 2.38 at 10 μm , this leads to a 16.7% reflection loss at the diamond-air interface and to a 8.0% loss at the diamond-water interface. This causes a reduction in the laser power reaching the aqueous sample between 16.7% and 24.7%, which needs to be taken into account for absolute PA measurements.

III. EXPERIMENTAL SETUP AND PA CELL DESIGN

The experimental setup used is shown in Fig. 3. As a light source for PA signal generation, either an external-cavity quantum-cascade laser (EC-QCL) (Daylight Solutions DLS-TLS-001-PL) or a CO_2 laser (Edinburgh Instruments PL3) was used. The EC-QCL is tunable over the wavelength range between 1005 and 1100 cm^{-1} , which overlaps with the two strong glucose absorption peaks. The CO_2 laser serves

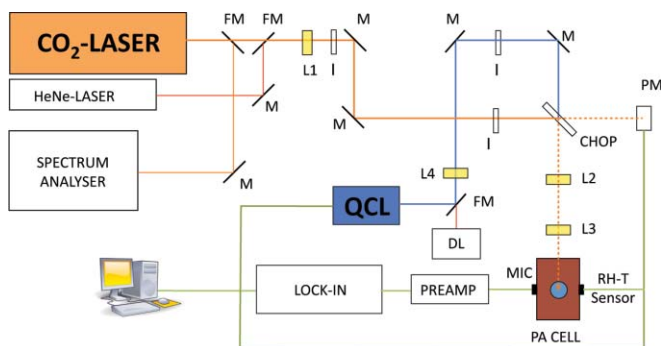


FIG. 3. (Color online) Setup for the photoacoustic measurements with the EC-QCL and CO_2 laser (M = mirror, FM = flipping mirror, L = lens, I = Iris, DL = diode laser, CHOP = chopper, PM = power meter, MIC = microphone, RH-T = relative humidity-temperature).

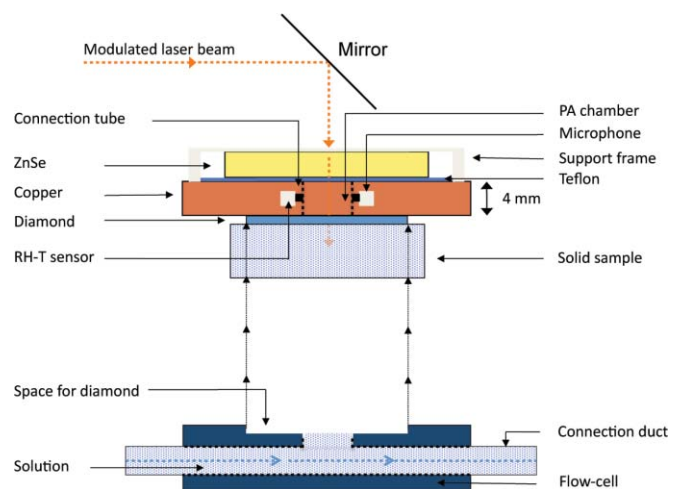


FIG. 4. (Color online) Schematic view of the photoacoustic cell closed with a diamond window and the flow cell (depicted below), which can be attached for the study of liquid samples.

for reference measurements at a wavelength with negligible glucose absorption around 940 cm^{-1} . Both continuous wave laser beams are modulated by a mechanical chopper (New Focus Model 3501). The chopper wheel is gold coated on both sides, in order to measure the reflected light with a pyroelectric sensor (Ophir Laserstar). Three ZnSe lenses are used to focus the laser beams into the PA cell. The red diode laser and the HeNe laser are used for alignment purposes. The PA signal is generated in the sample and the thermal wave is transferred via the diamond window (Diamond Materials) to the coupling gas inside the PA chamber, where the acoustic wave is detected with an electret microphone (Knowles FG-23329-P07). The microphone has a diameter of only 2.59 mm and a flat response from 100 Hz to 10 kHz with a sensitivity of 53 dB (relative to 1.0 V/0.1 Pa). The preamplified microphone signal is transferred to a lock-in amplifier (Stanford Research SR 830) and recorded with a computer. In addition to the PA measurements, the temperature and the relative humidity (RH) in the PA cell were recorded with a sensor (Sensirion SHT21, 3 mm \times 3 mm \times 1.1 mm), which provides an accuracy of ± 0.4 K and $\pm 3\%$ in RH.

A schematic of the transversal cross section of the PA cell is displayed in Fig. 4. The modulated laser beam enters the PA chamber at normal incidence through an AR coated ZnSe window, traverses the cell and leaves the chamber through a CVD diamond cover (either a 163 μm thick DW or a 3.91 μm thick diamond membrane (DM) with silicon support ring), which is in the direct contact with the sample of interest. The PA cell is fabricated out of copper and has a volume of only 78.5 mm^3 (radius $r = 2.5$ mm and length $L = 4$ mm). The inner surface was polished and gold coated to reduce undesired background cell signals. Two holes are drilled into the copper block from the left and the right side in which the microphone and the temperature-humidity sensor are placed. Both devices are connected via a 1 mm long tube (1 mm in diameter) with the PA chamber.

In order to study liquid samples, a flow cell can be conveniently attached to the PA cell (Fig. 4). The liquid is pumped from a reservoir through silicone tubes to the flow cell and

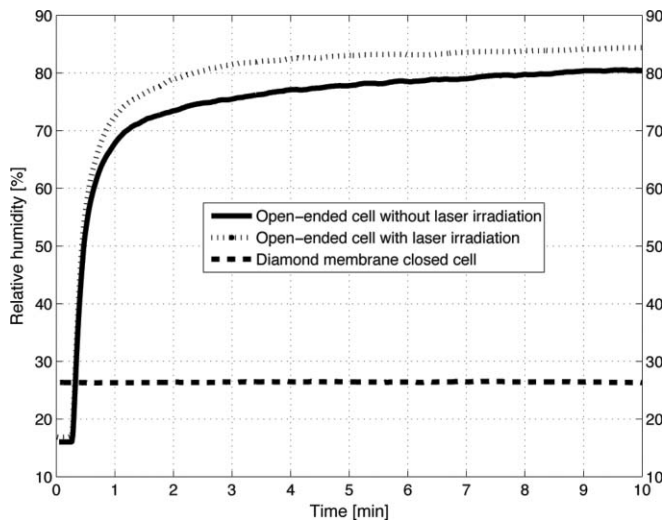


FIG. 5. Time dependence of the relative humidity in the photoacoustic chamber for the open-ended and the diamond-closed cell. A laser power of 21 mW was used for the measurement with the open-ended PA cell and 70 mW with the diamond membrane-closed PA cell.

back. The 5 mm diameter duct of the flow cell is separated from the PA chamber by the DW. The flow cell permits a continuous monitoring of liquid samples under varying conditions (e.g., concentration changes of a solute) without the need of sample exchanging. This leads to very stable measurement conditions. However, the pumping even at low rates of 60 ml/min causes mechanical vibrations of the PA cell. Hence, to increase the detection limit of a solute further the pumping was interrupted during short measurement intervals of ~ 1 min, which increased the signal-to-noise ratio (SNR) by a factor of 2 to 3.

IV. RESULTS AND DISCUSSION

A. Relative humidity and temperature in the PA cell

During measurements on the gelatine samples (5 g/dl gelatine in distilled water), the RH and the temperature within the PA cell have been recorded. The RH in the open-ended PA cell increases after placing it on the sample as Fig. 5 shows and reaches values of over 80% within 10 min even in the absence of laser irradiation. Operating the quantum-cascade laser (QCL) at moderate powers (i.e., 21 mW) further accelerates the evaporation of water. The increasing RH causes not only changes in the coupling gas but also leads to condensation on the ZnSe entrance window and the cell walls, which results in additional undesired background PA cell signals. Closing the PA cell with either the DW or the DM ensures stable conditions in the PA chamber even if the laser is operated at a power level of 70 mW (see Fig. 5). This makes the diamond-closed PA cell suitable for the study of aqueous solutions, gels, and outgassing samples.

The simultaneous monitoring of the temperature evolution during PA measurements did not lead to any significant variations in the temperature neither for the open-ended cell nor for the diamond-closed PA cell.

B. PA cell closed with DW

The first PA cell is closed with a $163 \mu\text{m}$ thick DW. Since the DW was not AR coated, it acts as a Fabry-Perot etalon with a wavelength-dependent transmission. The period between the transmission maxima is $\sim 13 \text{ cm}^{-1}$ which was taken into account for power normalization of the PA signal. The DW is robust and allows the study of a broad range of samples reaching from liquids to solids. Moreover, it can be used in conjunction with the flow cell since it sustains the pumping pressure.

The PA signal from a gelatine sample (5 g/dl gelatine dissolved in distilled water) was measured with the open-ended and the DW-closed PA cell in dependence of the QCL power at 1055 cm^{-1} using a 317 Hz modulation frequency (Fig. 6). As expected (Eq. (2)), the PA signal for both cells is proportional to the laser power. Despite the high thermal conductivity of CVD diamond, the insertion of the DW still leads to an ~ 6.5 times weaker signal amplitude compared to that of the open-ended PA cell. This is partially due to the horizontal heat transfer in the CVD DW away from the heat source, which increases the heated area but reduces the temperature maximum at the inner diamond surface. However, if a gelatine sample is investigated with the open-ended cell even under irradiation with only 15 mW average power, the sample gets damaged. If the DW-closed cell is used to investigate a gelatine sample no damage occurs even at laser powers exceeding 80 mW. This is due to the fact that the DW efficiently conducts the heat away from the irradiated area and, thereby, reduces longtime heating. Hence, the effect of weaker PA signals associated with the DW-closed cell can be partially compensated by using higher laser powers. The ratio of the power-normalized PA signals of the two cells is almost independent of the laser power (Fig. 6).

C. Photoacoustic cell closed with DM

The large amplitude drop of the PA signal caused by the lateral heat transfer can be circumvented by using a thin DM

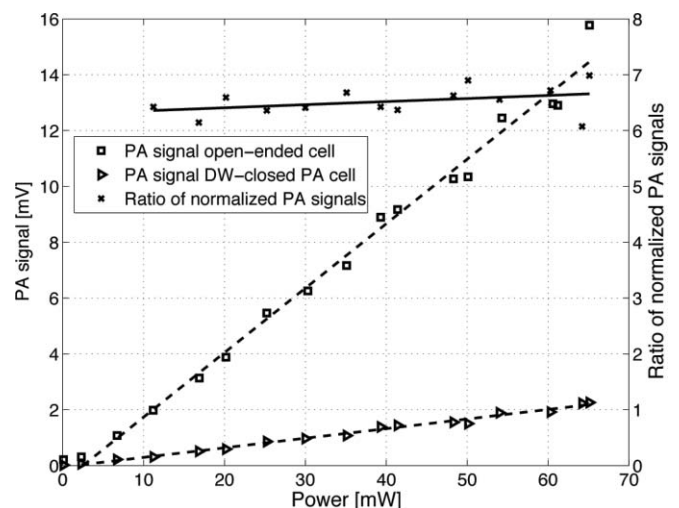


FIG. 6. PA signal of a gelatine sample vs laser intensity for the open-ended (\square) and the diamond window (DW)-closed PA cell (\triangleright) measured at 1055 cm^{-1} . The symbol (\times) denotes the ratio of the power-normalized PA signals of both cells.

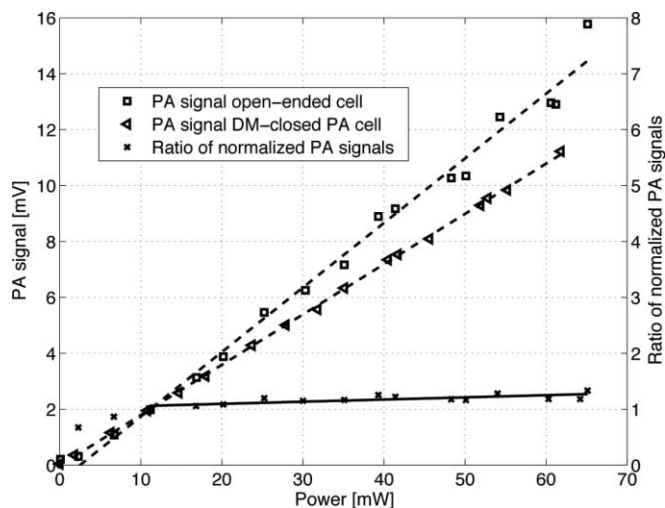


FIG. 7. PA signal of distilled water vs laser intensity for the DM-closed PA cell (\triangleleft) and the PA signal of a gelatine sample vs laser intensity for the open-ended (\square) PA cell, both measured at 1055 cm^{-1} . The symbol (\times) denotes the ratio of the power-normalized PA signals of both cells.

instead of the DW. As the DW, the DM was not AR coated and hence shows a wavelength-dependent transmission but with a much larger period (i.e., 537 cm^{-1}). The thickness of the DM has been selected as $3.91\text{ }\mu\text{m}$, adjusted to a transmission maximum within the QCL tuning range. The DM shortens the distance between the sample and the coupling gas by a factor of 42 in comparison with the DW and hence ensures an improved thermal contact. Moreover, the lateral heat transfer is substantially reduced which leads to stronger PA signals. Since the thin DM is very fragile, only liquids have been studied with this cell design by bringing the DM in direct contact with the liquid sample. It has not been tried to use the DM in conjunction with the flow cell since it might not sustain the pumping pressure.

The PA signal of distilled water has been measured with the DM-closed PA cell in dependence of the QCL power at 1055 cm^{-1} (see Fig. 7). As expected, a linear relationship between the magnitude of the PA signal and the laser power has been observed. When comparing the amplitudes of the PA signal obtained from the gelatine samples measured with the open-ended cell to those acquired from water samples measured with the DM-closed cell, only very small differences have been found. Hence, the signal strength obtained with the DM-closed cell almost reaches that of the open-ended cell as the ratio of 1.2 between the two configurations implies. A direct comparison of the PA signals from water and gelatine samples at 1055 cm^{-1} is justified, since the gelatine and water samples generate almost identical PA signals. This was demonstrated with corresponding measurements with the DW-closed PA cell, with which both gels and liquids can be investigated.

D. Glucose detection

The DW-closed PA cell has been used in conjunction with the flow cell to monitor time-dependent concentration changes of glucose dissolved in distilled water. Figure 8

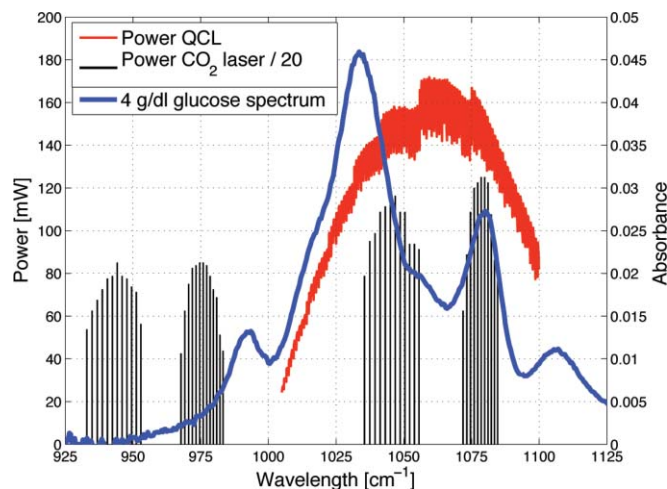


FIG. 8. (Color online) Spectrum of a 4 g/dl glucose solution with subtracted water background measured with a FTIR spectrometer and the output power of the EC-QCL and CO_2 laser in the wavelength range of interest.

shows the spectrum of glucose and the tuning range of the two lasers. The EC-QCL is tunable over the wavelength range of strong glucose absorption with the two absorption maxima at 1034 and 1080 cm^{-1} . Since the EC-QCL does not maintain a constant length of the laser cavity when the grating is rotated, mode-hops occur approximately every 0.9 cm^{-1} . By heating and cooling the laser cavity via a thermoelectric cooler, an almost continuous fine tuning of the laser emission becomes possible. The line tunable CO_2 laser serves as a reference at a wavelength around 940 cm^{-1} where glucose exhibits no absorption.

Fifty milliliters of distilled water were filled into the reservoir of the pumping system and pumped at a low pumping speed (60 ml/min) through the flow cell, to minimize mechanical vibrations of the PA cell. The glucose concentration was gradually increased by adding a previously prepared highly concentrated glucose (D-(+)-Glucose, Sigma Aldrich) solution to the water. When a homogeneous concentration throughout the liquid has been reached, pumping was stopped to reduce noise and 600 measurement points were recorded and averaged. A nearly linear increase of the PA signal with glucose concentration is observed when measuring close to the glucose absorption maximum at 1033 cm^{-1} (Fig. 9). The error-bars correspond to twice the standard deviation, i.e., $\pm\sigma$, using a lock-in integration time of 3 s. The signal has been normalized with respect to the signal obtained from pure distilled water. This yields a detection limit for glucose of 100 mg/dl for a SNR equal to 3. Due to the relatively small amplitude of the PA signal, ambient noise currently limits the detection threshold. A reference measurement with the CO_2 laser at 942 cm^{-1} shows, as expected, a constant PA signal if the glucose concentration is increased. The power fluctuation of the CO_2 laser, however, causes a larger measurement uncertainty.

It is the pumping system which determines the time resolution of the measurement, not the PA technique itself. After adding highly concentrated glucose solution, usually a disproportional large signal increase is seen, due to an inhomogeneous distribution of glucose throughout the liquid.

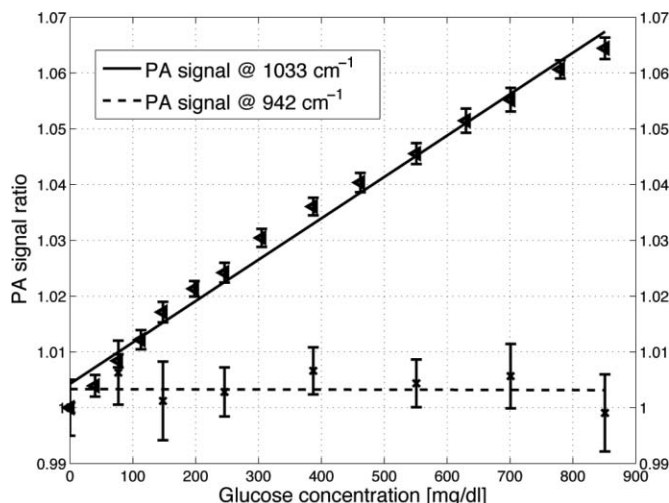


FIG. 9. Dependence of the PA signal on glucose concentration measured at 1033 cm^{-1} with the QCL and at 942 cm^{-1} with the CO_2 laser normalized with respect to the signal of pure distilled water. The error-bars correspond to $\pm\sigma$ (3 s integration time).

Depending on the amount of liquid as well as on the pumping speed of the system, the time needed to establish a homogeneous concentration and a stable PA signal varies, but it is typically shorter than 1 min.

E. Mutorotation of glucose

Combining the tuning possibilities of the EC-QCL with the properties of the DM-closed PA cell permits the recording of time-dependent spectra of liquid samples. When tuning the EC-QCL via the external grating the wavelength changes in steps of $\sim 0.9\text{ cm}^{-1}$. To record a spectrum, the grating position is tuned in small steps. The step size is chosen so small that the wavelength only changes every third step. So for every emission wavelength, three measurement series (corresponding to three different grating positions) consisting of 50 mea-

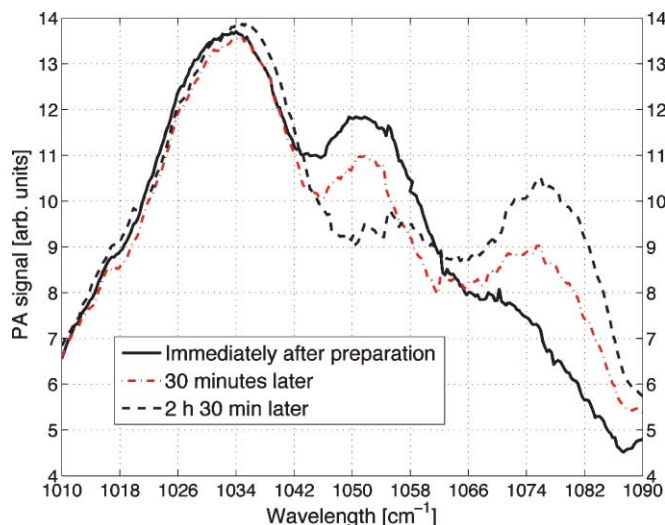


FIG. 10. (Color online) Time-dependent spectral changes of α -D-glucose powder dissolved in water due to mutorotation. The water background has been subtracted.

surement points could be recorded. The measured values have then been smoothed using a moving average. The spectrum of a glucose solution of 4 g/dl recorded immediately after preparation, 30 min later and 2.5 h later each with subtracted water background is shown in Fig. 10. α -D-glucose powder was used to prepare the solution. Dissolved in water, it reacts via mutarotation towards an equilibrium in which a ratio of about 36.4% α -D to 63.6% β -D-glucose is found.²⁵ This process is observed in Fig. 10 as it causes a temporal change in the glucose spectrum. In the initial spectrum (solid line), one observes two absorption maxima at 1034 and 1054 cm^{-1} . The absorption maximum at 1054 cm^{-1} gradually decreases over time while another one at 1080 cm^{-1} builds up.

V. CONCLUSION

The PA cell closed with a DW or DM ensures stable conditions in the PA chamber, which is necessary when sensitive measurements of liquids, gels, or outgassing samples need to be conducted. Moreover, the thermal and optical properties of diamond ensure strong PA signals. The optical transparency of CVD diamond reaching from 250 nm to the far-infrared offers a broad application field. However, a drawback of both the DW and the DM is their high price, but cheap alternatives such as plastic wrap made out of low density polyethylene did not yield satisfying results. Furthermore, a very thin DM is not perfectly flat. When a sample is placed on a membrane it may slightly change its curvature, so care has to be taken when changing the sample.

The DW-closed PA cell yields a robust setup for studies of liquids, gels, and solids. Combining the DW-closed cell with a flow cell represents a powerful tool to continuously investigate liquid samples under stable conditions. Applying this technique to the measurement of glucose content in aqueous solution has led to a detection limit of 100 mg/dl (for SNR 3). These measurements are currently limited by ambient noise due to the small PA signal amplitude. The detection limit would allow to measure glucose concentrations within the physiological range of humans (30-500 mg/dl). But for on-line non-invasive monitoring of glucose concentrations of diabetes mellitus patients, an improvement by a factor 5 is still needed. However, a possible industrial application for such a PA cell design with the current detection limit would be the on-line monitoring of glucose in beverages during production.

The PA cell design would be as well suitable for the study of suspensions, but then a constant pumping is required to investigate them under steady state conditions. If the pumping is stopped, the sedimentation process could be monitored time-resolved.

The DM-closed PA cell yields signal amplitudes comparable to those of the open-ended cell. The unique feasibility of the DM-closed cell to monitor time-resolved spectral changes has been demonstrated by studying the equilibrium reaction of α -D-glucose dissolved in water. Due to the fragility of the membrane, however, only liquid samples were investigated in this study.

So far only glucose dissolved in water has been investigated with the different diamond-closed PA cells. However, such a design is, in principle, applicable to any liquid or

solute showing a distinct absorption signature within the transmission range of diamond.

ACKNOWLEDGMENTS

The authors gratefully acknowledge the financial support from GlucoMetrix NIB and Non Invasive Diagnostic GmbH and the ETH Zurich.

- ¹K. Uchiyama, K. Yoshida, X.-Z. Wu, and T. Hobo, *Anal. Chem.* **70**, 651 (1998).
- ²R. Takamoto, S. Yamamoto, R. Namba, M. Matsuoka, and T. Sawada, *Anal. Chem.* **299**, 387 (1995).
- ³K. Giese, A. Nicolaus, B. Sennhenn, and K. Kölmel, *Can. J. Phys.* **64**, 1139 (1986).
- ⁴V. A. Fishman and A. J. Bard, *Anal. Chem.* **53**, 102 (1981).
- ⁵M. V. Marquezini, N. Cella, A. M. Mansanares, H. Vargas, and L. C. M. Miranda, *Meas. Sci. Technol.* **2**, 396 (1991).
- ⁶L. F. Perondi and L. C. M. Miranda, *J. Appl. Phys.* **62**, 1 (1987).
- ⁷L. Mota, R. Toledo, F. A. L. Machado, J. N. F. Holanda, H. Vargas, and R. T. Faria, Jr., *Appl. Clay Sci.* **42**, 168 (2008).
- ⁸A. Rosencwaig, *Rev. Sci. Instrum.* **48**, 1133 (1977).
- ⁹M. Ohmukai, H. Mukai, and Y. Tsutsumi, *Physica B* **394**, 132 (2007).
- ¹⁰M. Silva, I. N. Bandeira, and L. C. M. Miranda, *J. Phys. E: Sci. Instrum.* **20**, 1476 (1987).
- ¹¹K. Julliard, N. Gisin, and J.-P. Pellaux, *Appl. Phys. B* **65**, 601 (1997).
- ¹²J. A. Balderas-López, *Rev. Sci. Instrum.* **78**, 064901 (2007).
- ¹³A. Sikorska and B. B. Linde, *Chem. Phys.* **354**, 148 (2008).
- ¹⁴A. Sikorska, B. B. J. Linde, and W. Żwirbla, *Chem. Phys.* **320**, 31 (2005).
- ¹⁵A. Landa, J. J. Alvarado-Gil, G. Gutiérrez-Juárez, and M. Vargas-Luna, *Rev. Sci. Instrum.* **74**, 377 (2003).
- ¹⁶O. Delgado-Vasallo, A. C. Valdés, E. Marin, J. A. P. Lima, M. G. da Silva, M. Sthel, H. Vargas, and S. L. Cardoso, *Meas. Sci. Technol.* **11**, 412 (2000).
- ¹⁷D. H. McQueen, *J. Phys. E: Sci. Instrum.* **16**, 738 (1983).
- ¹⁸D. Bicanic, M. Chirtoc, I. Chirtoc, J. P. Favier, and P. Helander, *Appl. Spectrosc.* **49**, 1485 (1995).
- ¹⁹D. Bicanic, M. Anese, S. Luterotti, D. Dadarlat, J. Gibkes, and M. Lubbers, *Rev. Sci. Instrum.* **74**, 687 (2003).
- ²⁰S. L. Cardoso, C. M. F. Dias, J. A. P. Lima, M. S. O. Massunaga, M. G. da Silva, and H. Vargas, *Rev. Sci. Instrum.* **74**, 712 (2003).
- ²¹A. Rosencwaig and A. Gersho, *J. Appl. Phys.* **47**, 64 (1976).
- ²²H. D. Downing and D. Williams, *J. Geophys. Res.* **80**, 1656 (1975).
- ²³B. Dischler and C. Wild, *Low-Pressure Synthetic Diamond*, edited by H. Warlimont and E. Weber (Springer-Verlag, Heidelberg, Berlin, 1998).
- ²⁴E. Wörner, C. Wild, W. Müller-Sebert, M. Grimm, and P. Koidl, *Diamond Relat. Mater.* **14**, 580 (2005).
- ²⁵D. M. Back, D. F. Michalska, and P. L. Polavarapu, *Appl. Spectrosc.* **38**, 173 (1984).